iTRAQ-based proteomic analysis reveals the effect of ribosomal proteins on essential-oil accumulation in *Houttuynia cordata* Thunb.

Dandan Guo[1,2,*], Beixuan He[3,*], Fei Feng[1], Diya Lv[1,2], Ting Han[1] and Xiaofei Chen[1,2]

[1] School of Pharmacy, Naval Medical University, Shanghai, China
[2] Shanghai Key Laboratory for Pharmaceutical Metabolite Research, Shanghai, China
[3] State Key Laboratory of Oncogenes and Related Genes, Shanghai, China
[*] These authors contributed equally to this work.

ABSTRACT

Houttuynia cordata Thunb., also known as Yuxingcao in Chinese, occupies a pivotal role in Asian traditional medicine and cuisine. The aerial parts and underground stems of *H. cordata* exhibit remarkable chemical diversity, particularly in essential oil. Nevertheless, the mechanisms regulating essential oil biosynthesis in *H. cordata* remain unclear. In this study, we present a quantitative overview of the proteomes across four tissues (flower, stem, leaf, and underground stem) of *H. cordata*, achieved through the application of the isobaric tag for relative and absolute quantitation (iTRAQ). Our research findings indicate that certain crucial ribosomal proteins and their interactions may significantly impact the production of essential oils in *H. cordata*. These results offer novel insights into the roles of ribosomal proteins and their associations in essential oil biosynthesis across various organisms of *H. cordata*.

Subjects Agricultural Science, Biochemistry, Plant Science
Keywords *H. cordata*, iTRAQ, Proteomics, Ribosomal proteins, Essential-oil

Submitted 14 February 2024
Accepted 15 May 2024
Published 17 June 2024

Corresponding author
Xiaofei Chen, xfchen2010@163.com

Academic editor
Altijana Hromić-Jahjefendić

Additional Information and Declarations can be found on page 12

DOI **10.7717/peerj.17519**

INTRODUCTION

The history of herbal medicine is rich and spans various cultures. It is notable that numerous contemporary pharmaceuticals were originally derived from these medicinal plants (*Drasar & Khripach, 2019*). As interest in the application of medicinal plants continues to grow, there is a pressing need for the analysis of frequently utilized botanical remedies. A multitude of herbs exhibiting a "medicine-food homology", which ensures their safety for clinical use, have been meticulously investigated on a global scale (*Hou & Jiang, 2013*). *H. cordata*, a perennial herbaceous plant categorized under the *Saururaceae* family, is known to thrive in the damp and shaded locales of southwestern China. In traditional Chinese medicine, various parts of *H. cordata* are employed to alleviate swelling and pain, reduce inflammation, suppress coughs, and enhance diuretic effects (*Wu et al., 2021b*). Furthermore, the rhizomes and tender leaves of the plant are gathered as delectable spices and nutritious vegetables. Recent research has revealed its diverse array of attributes,

including anti-allergic, anti-inflammatory, antiviral, antioxidant, anti-leukemic, and anti-cancer properties (*Chen et al., 2013*; *Chiang et al., 2003*; *Kim et al., 2001*; *Li et al., 2005*; *Lu et al., 2006b*; *Ng et al., 2007*; *Zhuang et al., 2015*). These diverse pharmacological activities are frequently linked to the chemical composition of *H. cordata*, which encompasses a range of compounds, including alkaloids, essential oils, and flavonoids (*Bauer et al., 1996*). Moreover, the bioactivities of *H. cordata*'s oil have been documented since 1921, including decanoyl acetaldehyde, myrcene, ethyl decanoate, ethyl dodecanoate, and more (*Xu, 2012*). The extraction methods, bioactivity, and distribution pattern of *H. cordata*'s essential oil has been studied for nearly a century. There was an obvious difference observed between the aerial stems and the underground parts, with elevated levels of 2-undecanone, myrcene, ethyl decanoate, ethyl dodecanoate, 2-tridecanone, and decanal. Additionally, 11 constituents were exclusively isolated from the leaves, whereas seven of the identified components in the underground-stems were absent from the leaves (*Verma et al., 2017*). As previously stated, numerous studies have been conducted on the chemidiversity and spatial distribution pattern of essential oils *in vivo* (*Lin et al., 2022*; *Řebíčková et al., 2020*), as well as their pharmacological activities in *H. cordata* (*Wong et al., 2022*; *Wu et al., 2021a*). However, the key regulatory proteins or enzymes study involved in the biosynthesis of essential oils still remains unclear.

Isobaric tags for relative or absolute quantitation (iTRAQ), recognized as one of the premier mass spectrometry techniques for facilitating high-throughput proteomic analysis, offers the benefits of heightened sensitivity and robustness (*Evans et al., 2012*). iTRAQ has found extensive application across various domains including animals, plants, and microorganisms (*Baslam, Kaneko & Mitsui, 2020*; *Lü et al., 2021*). In recent times, iTRAQ analysis has been employed in some medical plants to investigate proteomic shifts in *Panax notoginseng* seeds (*Ge et al., 2021*), assess protein abundance in the underground stems of *Rehmannia glutinosa* (*Chen et al., 2021*), explore proteomic changes during the development haustorium of *Taxillus chinensis* (*Pan et al., 2022*), and conduct proteome profiling of *Anemone flaccida* (*Zhan et al., 2016*). However, iTRAQ has some limitations. Firstly, the commercial reagent is relatively expensive. Second, the maximum number of samples that can be labelled is limited. Thirdly, sample handling is complicated and time consuming. Finally, coverage of low abundance proteins can be poor (*Chen et al., 2021*; *Evans et al., 2012*). Despite these limitations, iTRAQ remains a valuable and powerful tool in quantitative proteomics.

The objective of this study is to employ iTRAQ proteomic technology to analyse the spatial proteome profiling of distinct medicinal parts in *H. cordata*. Furthermore, the correlation between protein expression patterns and essential oil accumulation across the distinct parts of *H. cordata* will be explored, thus deepening our comprehension of the molecular regulation mechanisms underlying their biosynthesis of essential oils.

MATERIALS AND METHODS

Plant material and sample source

H. cordata wild type plants were grown in medical plant garden of pharmacy college, Navy Medical University, under the natural climate. Different tissues samples for flower, stem,

leave and underground-stem were collected from flourishing plants in summer. They were put in a 1.5 ml tube and immediately in liquid nitrogen and stored at −80 °C until further use.

CDS library prediction

The RNA of flower, stem, leave and underground-stem tissues were extracted by Trizol kit as described. Total amounts and integrity of RNA were assessed by the RNA Nano 6000 Assay Kit of the Bioanalyzer 2100 system (Agilent Technologies, Santa Clara, CA, USA). cDNA library construction started with mRNA purification and then doble- strand cDNA synthesis and was quantified to ensure the quality of library. The separate libraries are pooling equivalently according to the concentration of samples, then being sequenced by the use of the Illumina NovaSeq 6000. The transcriptome assembly was performed using Trinity software (version 2.6.6) (*Grabherr et al., 2011*). Several databases were used to annotate gene functional annotation: Nr (NCBI non-redundant protein sequences); Nt (NCBI non-redundant nucleotide sequences); Pfam (Protein family); KOG/COG (Clusters of Orthologous Groups of proteins); Swiss-Prot (A manually annotated and reviewed protein sequence database); KO (KEGG Ortholog database); GO (Gene Ontology).

CDS represents the sequence encoding protein. CDS prediction firstly is mapped into NR and Swissprot. protein library. If mapped successfully, the open reading frame (ORF) of the transcript is isolated and the coding region sequence is translated into amino acid sequence (5′–>3′). For the sequences without successfully, the ORF was predicted by TransDecoder (3.0.1) software.

Protein extraction

Protein extraction was carried out according to the protocol of *Isaacson et al. (2006)* with some modifications. Frozen tissues were homogenized with a plant-tissue grinder. Protein extraction buffer was added to the sample and mixed gently in a vortex for 5∼10 min. Adding two volume of phenol saturated with Tris–HCl (pH 8.0) to each sample and then mixing for 10 min, followed by centrifugation at 14,000 g for 10 min at 4 °C. The upper phenolic phase was picked and mixed with 1.2 volume of protein extraction buffer, and then centrifuged. The upper phenolic phase was again collected and mixed with pre-cooled 0.1M ammonium acetate in methanol, followed by the incubation for 6 h at −20 °C. The precipitate was obtained by centrifugation at 14,000 g for 10 min and washed 1–2 times by pre-cooled methanol. Then the precipitate was washed 2–3 times by acetone containing 0.07% β-Mercaptoethanol and dried at room temperature. Protein concentration was determined by the BCA method (*Smith et al., 1985*).

Protein digestion

Protein digestion was carried out according to the method of FASP (*Wiśniewski et al., 2009*). Dried protein powder sample was resolved in 8M urea with Tris-Hcl (pH 8.0). 1M reducing reagent (DTT) was added to cell protein lysates and incubated at 55 °C for 1 h, followed by 5 μL 1M cysteine-blocking reagent (IAA) for 30 min at 25 °C in dark. Then the samples were transferred into 10 KDa ultrafiltration tube and centrifuged 14,000 g for 15 min at 4 °C. Then 100 μL 8M urea was added twice to the ultrafiltration membrane

to protein denaturation completely. 0.5 M TEAB was added and centrifuged three times at 14,000 g for 15 min to clean denaturation reagent. Sequencing grade trypsin (Enzyme: Substrate = 1:50) was incubated with samples at 37 °C overnight. Next day, the peptide samples were collected and added 1% formic acid to stop the reaction.

iTRAQ labeling and high pH reverse phase separation by HPLC

The peptides were subjected to vacuum centrifugation to facilitate drying. Subsequently, the dried peptides were suspended in TEAB buffer and labeled by iTRAQ 8-plex kits in accordance with the manufacturer's instructions (AB SCIEX Inc., Framingham, MA, USA, AB SCIEX Inc., USA). The labeling reaction was initiated by the addition of a reagent vial to the digested peptides, which were then incubated at room temperature for a period of two hours. Following this, 100 μL of water was added to halt the reaction. The labeling scheme was as follows: The tags used were 113 and 114, F1 and F2; Tags 115 and 116, L1 and L2; Tags 117 and 118, S1 and S2; Tags 119 and 121, Us1 and Us2. Following this, all the samples were pooled for mass spectrometry analysis. High pH reverse phase separation by HPLC was performed in accordance with the previously decribed methodology (*You et al., 2017*), with certain modifications. The Agilent 1100 HPLC with Agilent Zorbax Extend C18 column (2.1 × 150 mm, 5 μm) were used for peptide separation at a flow rate of 1.0 ml/min. The mobile phases A was 20 mM ammonium formate (pH = 10), while the mobile phases B was 80% acetonitrile with 20 mM ammonium formate (pH = 10). The entire gradient course lasted for 65 min, with the following profile: 5 min at 5% B, 30 min at 15% B, 45 min at 38% B, 46 min at 90% B, 54.5 min at 90% B, 55 min at 5% B, and finally 65 min at 5% B.

LC–MS/MS analysis

Microflow LC-MS/MS analysis was conducted by coupling Eksigent Micro LC-1D plus system to Triple TOF 5600 System (AB SCIEX Inc., Framingham, MA, USA). Samples for the proteome analysis were resuspended in 2% acetonitrile containing 0.1% formic acid. Peptide loading and washing were done on a trap column (ChromeXP C18_CL-3 μm, 120A, 350 μm × 0.5 μm, AB,SCIEX) at a flow rate of 10 μL/min in 2% acetonitrile (0.1% formic acid) for 7 min. Peptide separation was performed on an analytical column (0.075 × 150 mm, 3 μm, 120A, AB SCIEX Inc.) at a flow rate of 5 μL/min using a 120 min gradient from 5% to 80% solvent B (solvent A: 2% acetonitrile with 0.1% formic acid in LC-MS grade water; solvent B: 98% acetonitrile with 0.1% formic acid in acetonitrile) for proteome analysis. A spray voltage of 2.3 kV and ESI ion source temperature of 150 °C were employed to facilitate the ionisation of peptides. A switch from MS to MS2 scanning was automatically initiated based on the data collected from the instrument. For the full proteome samples, full scan MS spectra (m/z 350–1,500) were acquired. In the Time of Fight detector, high-resolution MS2 spectra were acquired for the 40 most abundant precursor ions. This analysis was conducted with the objective of fragmenting precursors with charge states between 2 and 5.

Analysis of proteomic data

Peptide and protein identification and quantification data files were searched with Protein Pilot software (v.5.0) using default parameters (*Zhang et al., 2014*). MS/MS spectra were searched against CDS library (Hc. blast.pep.fasta). Trypsin was the only specific protease and iTRAQ-8-plex (peptide labelled) was chosen as sample labeling type (FDR $\leq$ 1%). The annotations of the identified proteins, combined with the result of BLAST alignments. The screening criteria for differential expression proteins (DEPs) was |Fold Change (FC)| $\geq$ 2 and a *p*-value $\leq$0.05 in aerial parts (Leaf, Stem, Flower) compared to underground -stem. The Weighted Gene CoExpression Network Analysisn (WGCNA) of identified proteins was performed with the R package WGCNA (https://cran.rstudio.com/web/packages/WGCNA), and further bioinformatic analysis of DEP was performed using the OECloud tools (https://cloud.oebiotech.cn/), based on the Gene Ontology (GO) categories and KEGG Ortholog database.

Bioinformatic analysis of different expression proteins

The KEGG pathway enrichment profile of DEPs was analyzed by OECloud tools with FDRs less than 0.05, and DEPs data was displayed using volcano plots and Wayne diagram with the help of the image GP. The prediction of functional protein association networks was analyzed by the STRING database (http://string-db.org/).

RESULTS

Plant morphology and chemical composition

The general morphology of the *H. cordata* plant during its flowering period is illustrated (Fig. 1A). The plant is divided into four sections: flowers, stems, leaves, and underground stems (Us). Flowers, stems, and leaves are classified as aerial parts (AP). Medicinal components application in both AP and Us, were recognized for their heat-clearing and detoxifying properties in traditional Chinese medicine. Among the constituents of *H. cordata* essential oil, the most predominant compounds were 2-undecanone (23.96–36.07%), β-myrcene (12.57–14.29%), bornyl acetate (6.03−8.61%), and β-pinene (trace - 23.29%) (chemical structures shown in Fig. 1B). The previous findings indicated that the essential oil content is higher in the aerial parts of *H. cordata* compared to its underground stems (*Lu et al., 2006a*). These findings suggest that the substantial variation of essential oil content could potentially be linked to the differential expression of proteins across distinct plant parts in *H. cordata*.

Assembled transcriptome analysis

To perform proteomics analysis, RNA-seq is carried out to build non-model plant proteins identification search database. Based on transcriptome result, 90,067 transcripts were assembled in tissues pool (flower, stem, leave and underground-stem) of *H. cordata*, of which 33,493 were unigenes that represents the longest transcript of each gene. More than 50% of unigenes were distributed between 300–1000 bp (Fig. S1A). 21,661 unigenes (64.67%) were annotated by Nr (NCBI non-redundant protein sequences) database, while annotated 13,290 unigenes were screened out by Nt (NCBI nucleotide sequences) database.

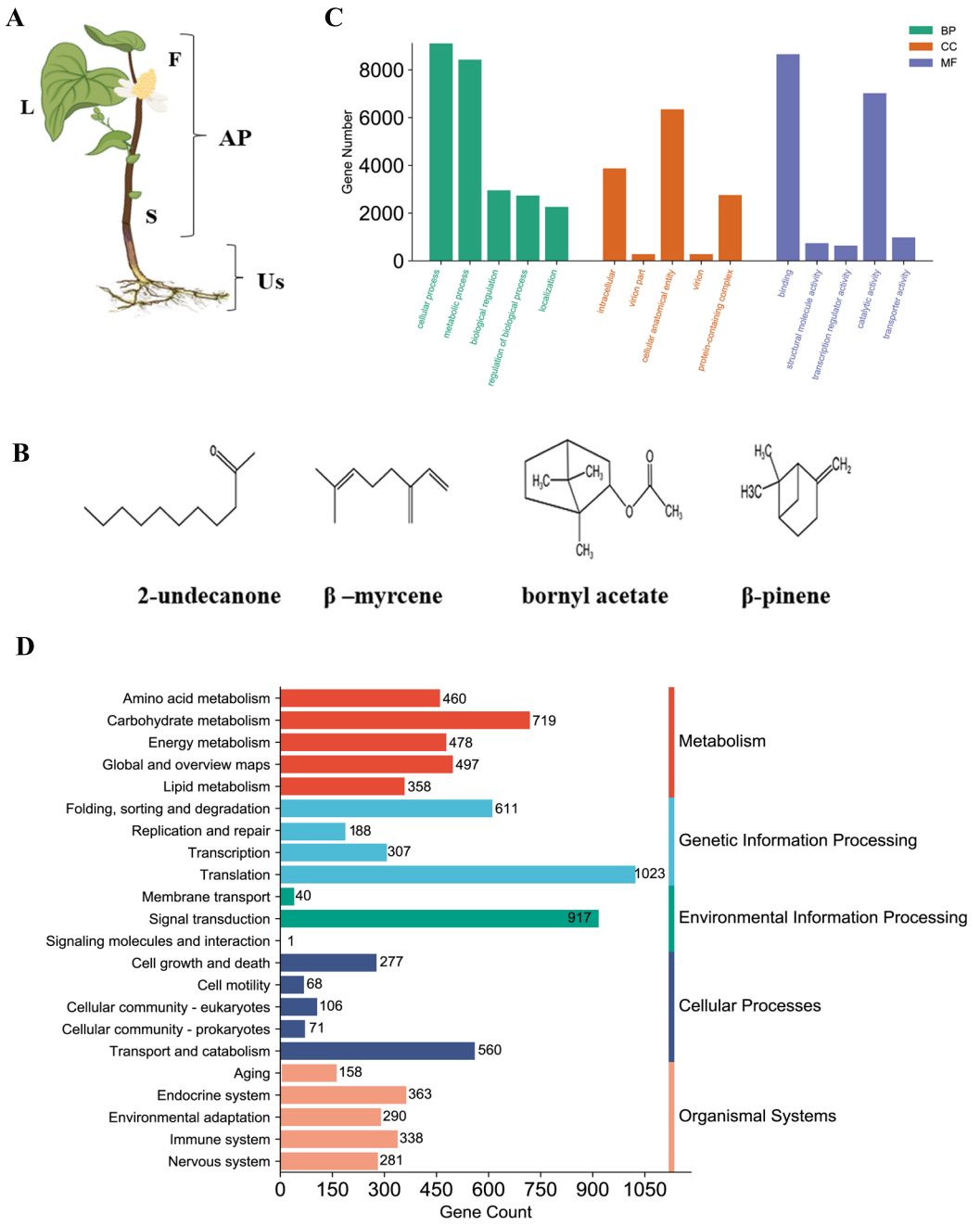

Figure 1 **Phenotype and chemical components and RNA-seq analysis of *H. cordata*.** (A) Tissue samples analyzed according to morphology group, F, Flower; S, Stem; L, Leaf; and Us, Underground-stem. AP, Aerial parts; Us, Underground-stem. This image was drawn following images available at the Plant Photo Bank of China: http://ppbc.iplant.cn/sp/15036. (B) Structures of the major chemical components of *H. cordata*. (C) GO annotation classification includes biological process (BP), cellular component (CC), molecular Function (MF). (D) KEGG pathway classification was divided into five branches.

Full-size DOI: 10.7717/peerj.17519/fig-1

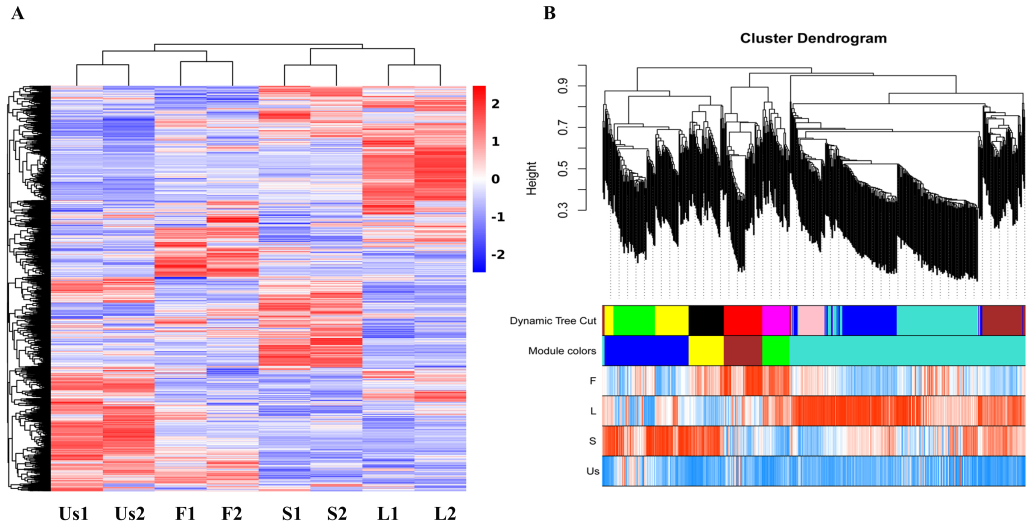

Figure 2 **Cluster maps of identified proteins in each tissue of *H. cordata*.** (A) Heatmaps of proteins in different tissues. (B) Visualization of WGCNA results.

Full-size DOI: 10.7717/peerj.17519/fig-2

15,756 were annotated by GO (Gene Ontology) and involved in cellular and metabolic process (Fig. S1B and Fig. 1C). 8,928 unigenes were mapped to KO and KEGG (Kyoto Encyclopedia of Genes and Genomes) pathway which mainly participated in translation and signal transduction (Figs. 1C and 1D). In total of 4,177 unigenes existed in multiple databases. 19,271 peptides sequence of CDS were predicted through Nr and SwissProt. Assembled transcriptome database serves as an extensive public repository, serving as a valuable search resource for proteomic studies of *H. cordata.*

Overview of proteomics analysis

The proteomics analysis identified a total of 3,261 proteins across the four parts (flower, stem, leaf, and underground-stem) of *H. cordata*. Notably, the expression clusters exhibited significant distribution shifts among the various plant parts, as shown in Fig. 2A. In terms of GO categories, 1,470 proteins were involved in biological processes, 1,194 proteins were linked to cellular components, and 2,247 proteins were associated with molecular functions (Fig. S2A). Moreover, 1,684 proteins were assigned to KEGG pathways, with 31 notable signalling pathways exhibiting significance (p value ≤ 0.05). The three leading pathways were those of dihydrolipoamide dehydrogenase, photosystem I P700 chlorophyll apoprotein A1, and the 26S proteasome complex subunit DSS1 (Fig. S2B). To assess the correlation coefficients among the expressed proteins across various parts of *H. cordata*, WGCNA analysis was conducted. This analysis classified the 3,930 proteins into five distinct modules, revealing correlations that ranged from high to low among the MEturquoise proteins. Notably, the proteins expressed in the underground-stem exhibited a lower correlation coefficient with those in the aerial parts (Fig. 2B and Fig. S3).

DEPs analysis of aerial parts and underground-stem

A significance cutoff was established with criteria including a fold change ≥ 1.5 and a p-value ≤ 0.05 (t-test), along with a false discovery rate of $\leq 1\%$. Compared with the proteins in underground-stem, 306 proteins were up-regulated in leaf, 192 were up-regulated in flower, and 266 were up-regulated in stem, there were 61 proteins increased both in leaf and stem (Fig. 3A). In comparison to the underground-stem, ribosomal proteins L23A and S28 displayed a notable upregulation in flower tissue. Similarly, proteins L1, L30e, L23A, L4, and L29 exhibited upregulation in both the stem and leaf. Conversely, P3-like and S8 were found to be downregulated in the stem and leaf (Figs. 3B–3D). Furthermore, the differential abundance proteins (DAPs) were associated with KEGG pathways, with 251 proteins being mapped to these pathways. Notably, this study revealed 12 significant signalling pathways (p-value ≤ 0.05), with the differentially expressed proteins (DEPs) being most prominently enriched within the large subunit ribosomal protein group (Fig. 3E). The findings suggest that large subunit ribosomal proteins might play a role in influencing essential oil accumulation in aerial parts (AP).

The expression profile of interesting proteins

In this study, a total of 34 ribosomal proteins were identified, including 10 small subunit ribosomal proteins and 24 large subunit ribosomal proteins (Table 1). The majority of these exhibited higher expression levels in the leaf and stem, a pattern consistent with the spatial distribution of active components (Fig. 4A) (*Lu et al., 2006a*). The internet analysis revealed that the majority of ribosomal proteins in *H. cordata* exhibited robust interactions with those in *Arabidopsis thaliana* according to STRING model data. (Fig. 4B, Table 1).

DISCUSSION

As is well known, leaves, stems, and underground-stems of *H. cordata* are of great importance in traditional Chinese medicine due to their application in heat-clearing and detoxification therapies. Moreover, distinct variations in chemical composition have been observed between different plant parts (*Verma et al., 2017*). The essential oil, which is the main active constituent, shows significant variation between the aerial and underground parts. However, the distinctive protein profiling, which forms the basis for subsequent investigations into molecular mechanisms, remains elusive. To shed light on the variation in protein expression in *H. cordata* tissues, a comparative proteomic analysis using iTRAQ was performed. A total of 306 and 266 differentially abundant proteins (DAPs) were successfully identified in the leaf and stem, respectively, which showed up-regulated expression compared to the underground stem. These DAPs were categorized according to their functions and were found to be enriched in pathways such as photosynthesis, glycolysis, and ribosomal processes. These findings provide the basis for the identification and functional analysis of potential proteins associated with the interspecific variation of essential oil in *H. cordata*.

The ribosome, an ancient, intricate, and complex organelle, maintains a remarkably conserved structure and composition across prokaryotes and eukaryotes (*Ramakrishnan & White, 1998*). In a eukaryotic cell, the ribosome comprises four ribosomal RNAs and

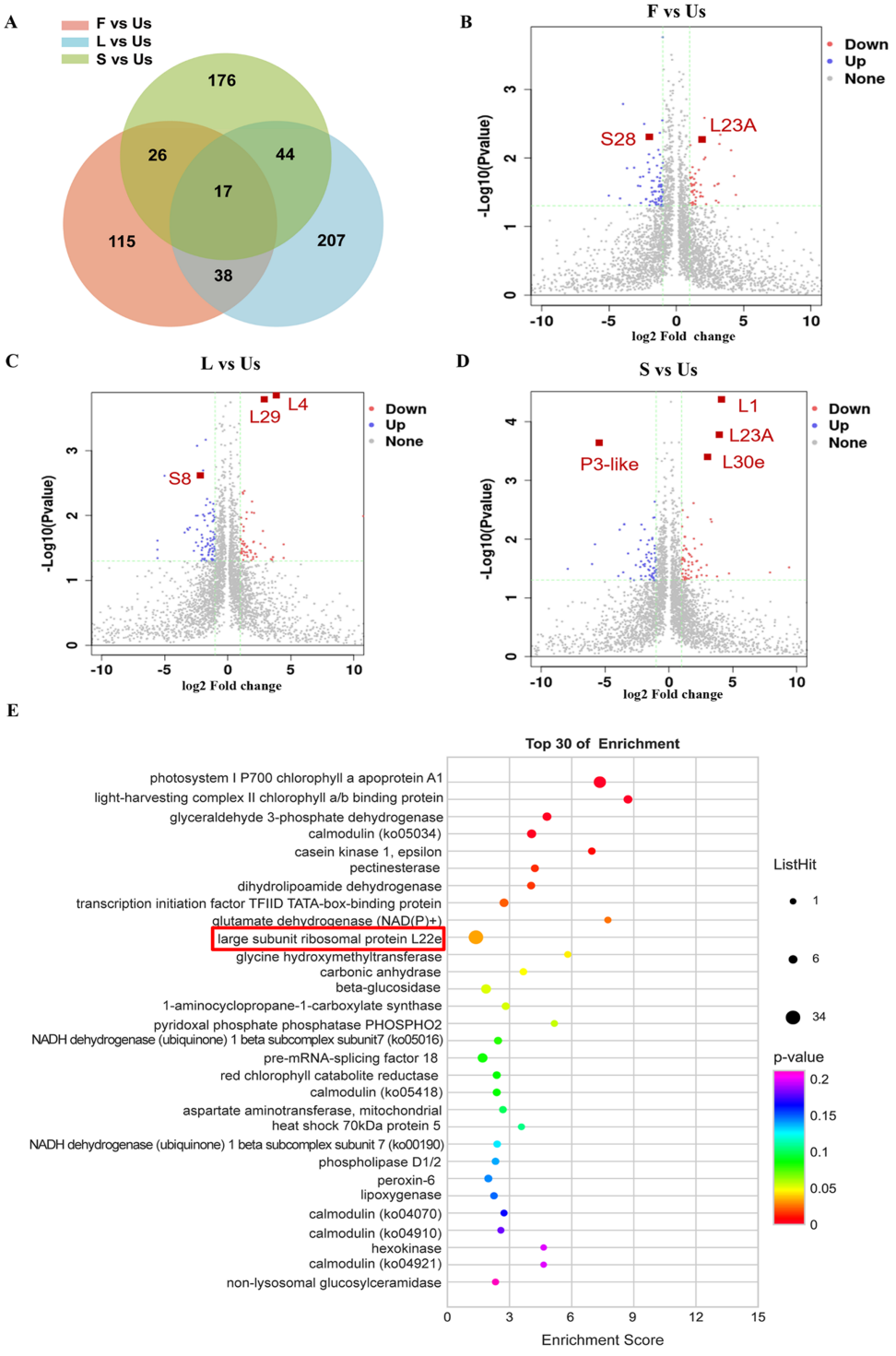

Figure 3 **Differentially expressed proteins analysis of different tissues in *H. cordata*.** (A) Venn diagrams showing the numbers of differentially expressed proteins. (B, C, D) Volcano plot of differentially expressed proteins ($n = 2$). (E) KEGG pathway enrichment analysis of differentially expressed proteins.
Full-size DOI: 10.7717/peerj.17519/fig-3

Table 1 Expression of ribosomal proteins in different tissues.

Accession	type	F	L	S	Us
Cluster-4666.13037	Small subunit ribosomal protein S5	0.587694	8.207778	4.26584	0.605816
Cluster-4666.5849	Small subunit ribosomal protein S6	0.858897	20.8466	2.611892	0.351564
Cluster-4666.12357	Small subunit ribosomal protein S3e	1.048239	1.852502	6.082382	2.13907
Cluster-4666.11333	Small subunit ribosomal protein S4e	1.593881	1.045695	7.180683	1.842053
Cluster-4666.14273	Small subunit ribosomal protein S8e	1.048239	0.630984	1.070769	0.520195
Cluster-4666.9797	Large subunit ribosomal protein L1	0.858897	10.89376	2.863531	0.125623
Cluster-4666.7389	Large subunit ribosomal protein L18	0.662544	1.847383	1.185969	0.707684
Cluster-4666.13864	Large subunit ribosomal protein L29	1.401509	11.81121	5.308409	0.411917
Cluster-4666.9022	Large subunit ribosomal protein L3	1.435341	3.710995	1.564803	1.024261
Cluster-4666.11140	Large subunit ribosomal protein L4	1.196579	5.888499	2.755063	0.103792
Cluster-4666.7056	Large subunit ribosomal protein L4	0.995416	2.374982	1.609338	1.068313
Cluster-4666.11973	Large subunit ribosomal protein LP1	0.91973	0.304113	0.117207	2.137985
Cluster-4666.14276	Large subunit ribosomal protein L13Ae	1.129462	0.894154	4.487644	1.125452
Cluster-4666.12344	Large subunit ribosomal protein L14e	0.879289	3.034696	7.178391	1.481314
Cluster-4666.11498	Large subunit ribosomal protein L18Ae	1.337471	0.559793	4.573985	1.273215
Cluster-4666.12924	Large subunit ribosomal protein L21e	1.033298	0.616777	7.188906	1.592887
Cluster-4666.11662	Large subunit ribosomal protein L23Ae	0.939511	0.470213	2.643782	0.228153
Cluster-4666.12502	Large subunit ribosomal protein L27Ae	1.37694	1.348457	2.301466	0.974233
Cluster-4666.11924	Large subunit ribosomal protein L28e	1	1.187894	2.329858	0.43075
Cluster-4666.15104	Large subunit ribosomal protein L4e	1.153085	0.678525	4.328074	1.181494
Cluster-4666.11447	Large subunit ribosomal protein L6e	0.977496	0.159101	2.885133	0.959655
Cluster-4666.12046	Large subunit ribosomal protein L7e	0.769755	1.196298	4.234263	1.93658
Cluster-4666.15918	Large subunit ribosomal protein L13e	2.418536	1.522815	14.21225	2.044358
Cluster-4666.12871	Small subunit ribosomal protein S3Ae	1.401509	0.511285	1.508379	0.184063
Cluster-4666.9242	Large subunit ribosomal protein L38e	1.677524	2.817341	7.806055	2.564219
Cluster-4666.13728	Large subunit ribosomal protein L11e	1.196579	0.524089	5.445374	1.426766
Cluster-4666.7689	Large subunit ribosomal protein L19	1.004627	2.652266	0.740199	0.140157
Cluster-4666.12018	Large subunit ribosomal protein L30e	0.951825	2.807338	10.42594	1.194464
Cluster-4666.12688	Small subunit ribosomal protein S15e	0.777313	0.29411	2.414225	0.819777
Cluster-4666.10888	Large subunit ribosomal protein L13	1.928795	11.23692	5.154253	1.219788
Cluster-4666.12692	Small subunit ribosomal protein S25e	1.095621	0.522402	0.965978	0.136825
Cluster-4666.12733	Large subunit ribosomal protein L5e	0.868952	0.507198	1.837785	0.3925
Cluster-4666.12390	Large subunit ribosomal protein L18e	1.242968	0.646883	2.356648	0.240595
Cluster-4666.3656	Small subunit ribosomal protein S24e	0.875811	0.746968	1.599829	0.571713

79-81 ribosomal proteins. It is widely acknowledged that ribosomal proteins contribute to the maintenance of RNA conformation (*Barakat et al., 2001*). Nevertheless, an increasing number of studies have uncovered that ribosomal proteins are not solely involved in rRNA processing, folding, assembly, and ribosomal subunit transportation, but also in the reinforcement of subunit architectures and the interaction between ribosomes and diverse translation factors. Furthermore, they contribute to the folding and positioning of nascent peptides and potentially possess additional biological functions beyond the ribosomal context (*Wilson & Doudna Cate, 2012*). To date,, only a limited number of studies have

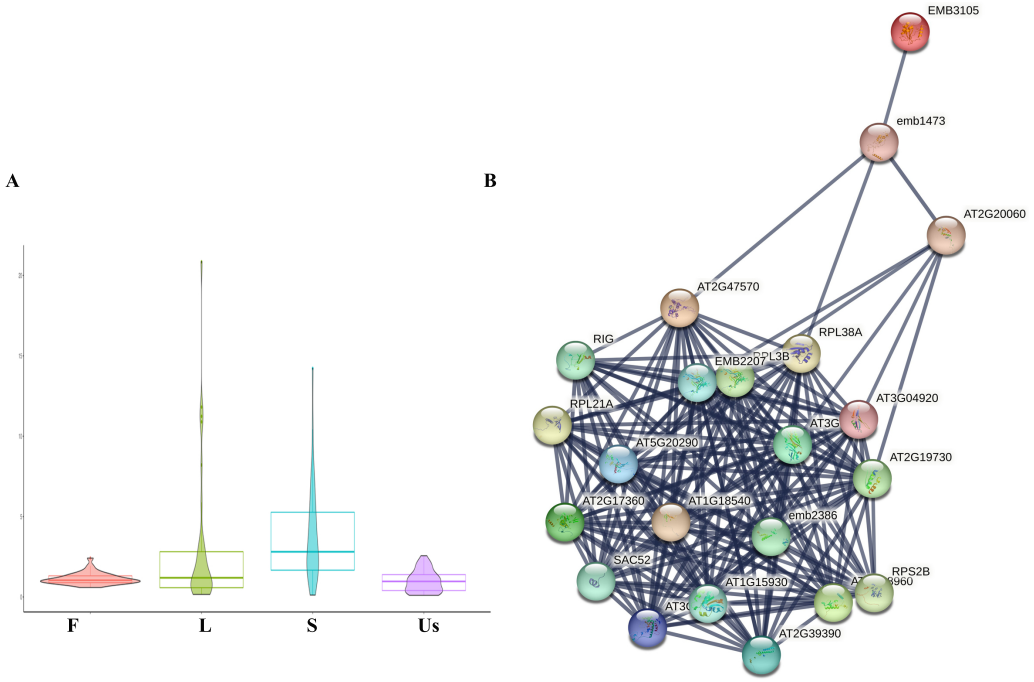

Figure 4 Differentially expressed analysis of ribosomal proteins. (A) Ribosomal proteins expression profiling in different tissues of *H. cordata*. (B) Interaction network of subunit ribosomal protein compared to *Arabidopsis thaliana* (confidence was set ≥0.9).

Full-size DOI: 10.7717/peerj.17519/fig-4

revealed the significant role of ribosomal proteins in essential oil accumulation, which may regulate the biosynthesis of secondary metabolites and even impact plant development and abiotic stress tolerance (*Wilson & Doudna Cate, 2012*). According to reports, ribosomal proteins uS2c, uS4c, bL20c, and bL33c have been demonstrated to influence abnormal leaf morphologies (*Rogalski et al., 2008*). Furthermore, ribosomal protein bS1c has been demonstrated to affect nuclear and plastid genes encoding proteins involved in chlorophyll biosynthesis, chloroplast development, and photosynthesis (*Gong et al., 2013*; *Zhou et al., 2021*). In addition, the tobacco's PRP bL33c plays a role in enhancing plant tolerance to low-temperature stress (*Rogalski et al., 2008*). PRP bS1c was observed to inhibit HsfA2-dependent heat stress responses in the chloroplasts of Arabidopsis (*Yu et al., 2012*).

Although considerable progress has been made in recent years, a comprehensive understanding of the individual functions of each PRP and their involvement in specific biological processes remains elusive. In the study, 18 upregulated Differentially Abundant Proteins (DAPs) were recognized as ribosomal proteins, encompassing large subunit ribosomal proteins L13, L19, and L3. Essential oils are defensive metabolites and physiological responses to environmental stress in *H. cordata* (*Zhou et al., 2021*). The essential oil of *H. cordata* contains a variety of components, some of which have significant medicinal value. Ribosomal proteins can directly affect the synthesis and accumulation of various components in the essential oil by regulating the expression of key genes or enzyme activities in the essential oil synthesis pathway. It is of great importance for the medicinal

efficacy and quality control of the medicinal components in *H. cordata*. In addition, *H. cordata* grows in a variable environment and is exposed to various biotic and abiotic stresses. Ribosomal proteins may be involved in the regulation of essential oil biosynthesis to adapt to changes in the external environment and improve stress resistance in *H. cordata*.

This research suggests that manipulation of ribosomal protein expression by biotechnological tools may be an effective strategy to stimulate essential oil biosynthesis in *H. cordata*. These findings provide the basis for guiding the utilization of seed resources and enhancing the chemical diversity of components in both the aerial parts and underground-stem of *H. cordata*.

CONCLUSION

In this study, we reported iTRAQ-based quantitative proteomics of *H. cordata*, identifying a total of 3,261 proteins and mapping the differential expression pattern across multiple tissues. By correlating analysis with essential oil content, our results demonstrated that ribosomal proteins could significantly influence essential oil production in *H. cordata*. The research provides a novel insight into the study of protein function involved in essential oil in non-model plants.

ACKNOWLEDGEMENTS

We acknowledge the assistance of staff at the Pharmaceutical Analysis and Testing center.

ADDITIONAL INFORMATION AND DECLARATIONS

Funding

This work was supported by the National Natural Science Foundation of China (No. 82104328 and 81973291) and the Sailing Program Science and Technology Commission of Shanghai Municipality (No. 20YF1458900). The funders had no role in study design, data collection and analysis, decision to publish, or preparation of the manuscript.

Grant Disclosures

The following grant information was disclosed by the authors:
The National Natural Science Foundation of China: 82104328, 81973291.
Sailing Program Science and Technology Commission of Shanghai Municipality: 20YF1458900.

Competing Interests

The authors declare there are no competing interests.

Author Contributions

- Dandan Guo conceived and designed the experiments, performed the experiments, analyzed the data, prepared figures and/or tables, authored or reviewed drafts of the article, and approved the final draft.

- Beixuan He analyzed the data, prepared figures and/or tables, authored or reviewed drafts of the article, and approved the final draft.
- Fei Feng performed the experiments, analyzed the data, prepared figures and/or tables, and approved the final draft.
- Diya Lv analyzed the data, prepared figures and/or tables, and approved the final draft.
- Ting Han analyzed the data, prepared figures and/or tables, and approved the final draft.
- Xiaofei Chen conceived and designed the experiments, authored or reviewed drafts of the article, and approved the final draft.

Data Availability

The following information was supplied regarding data availability:

The proteomics data of *H. cordata* is available at iProX: IPX0005722000.

Supplemental Information

Supplemental information for this article can be found online at http://dx.doi.org/10.7717/peerj.17519#supplemental-information.

REFERENCES

Barakat A, Szick-Miranda K, Chang IF, Guyot R, Blanc G, Cooke R, Delseny M, Bailey-Serres J. 2001. The organization of cytoplasmic ribosomal protein genes in the Arabidopsis genome. *Plant Physiology* **127**:398–415 DOI 10.1104/pp.010265.

Baslam M, Kaneko K, Mitsui T. 2020. iTRAQ-based proteomic analysis of rice grains. *Methods in Molecular Biology* **2139**:405–414 DOI 10.1007/978-1-0716-0528-8_29.

Bauer R, Pröbstle A, Lotter H, Wagner-Redecker W, Matthiesen U. 1996. Cyclooxygenase inhibitory constituents from houttuynia cordata. *Phytomedicine* **2**:305–308 DOI 10.1016/S0944-7113(96)80073-0.

Chen HY, Lin YH, Thien PF, Chang SC, Chen YC, Lo SS, Yang SH, Chen JL. 2013. Identifying core herbal treatments for children with asthma: implication from a chinese herbal medicine database in Taiwan. *Evidence-Based Complementary and Alternative Medicine* **2013**:125943.

Chen P, Wei X, Qi Q, Jia W, Zhao M, Wang H, Zhou Y, Duan H. 2021. Study of terpenoid synthesis and prenyltransferase in roots of rehmannia glutinosa based on iTRAQ quantitative proteomics. *Frontiers in Plant Science* **12**:693758 DOI 10.3389/fpls.2021.693758.

Chiang LC, Chang JS, Chen CC, Ng LT, Lin CC. 2003. Anti-herpes simplex virus activity of bidens pilosa and houttuynia cordata. *The American Journal of Chinese Medicine* **31**:355–362 DOI 10.1142/S0192415X03001090.

Drasar PB, Khripach VA. 2019. Growing importance of natural products research. *Molecules* **25**:6 DOI 10.3390/molecules25010006.

Evans C, Noirel J, Ow SY, Salim M, Pereira-Medrano AG, Couto N, Pandhal J, Smith D, Pham TK, Karunakaran E, Zou X, Biggs CA, Wright PC. 2012. An insight into iTRAQ: where do we stand now? *Analytical and Bioanalytical Chemistry* **404**:1011–1027 DOI 10.1007/s00216-012-5918-6.

Ge N, Yang K, Yang L, Meng ZG, Li LG, Chen JW. 2021. iTRAQ and RNA-seq analyses provide an insight into mechanisms of recalcitrance in a medicinal plant Panax notoginseng seeds during the after-ripening process. *Functional Plant Biology* **49**:68–88 DOI 10.1071/FP21197.

Gong X, Jiang Q, Xu J, Zhang J, Teng S, Lin D, Dong Y. 2013. Disruption of the rice plastid ribosomal protein s20 leads to chloroplast developmental defects and seedling lethality. *G3* **3**:1769–1777 DOI 10.1534/g3.113.007856.

Grabherr MG, Haas BJ, Yassour M, Levin JZ, Thompson DA, Amit I, Adiconis X, Fan L, Raychowdhury R, Zeng Q, Chen Z, Mauceli E, Hacohen N, Gnirke A, Rhind N, Di Palma F, Birren BW, Nusbaum C, Lindblad-Toh K, Friedman N, Regev A. 2011. Full-length transcriptome assembly from RNA-Seq data without a reference genome. *Nature Biotechnology* **29**:644–652 DOI 10.1038/nbt.1883.

Hou Y, Jiang JG. 2013. Origin and concept of medicine food homology and its application in modern functional foods. *Food & Function* **4**:1727–1741 DOI 10.1039/c3fo60295h.

Isaacson T, Damasceno CM, Saravanan RS, He Y, Catalá C, Saladié M, Rose JK. 2006. Sample extraction techniques for enhanced proteomic analysis of plant tissues. *Nature Protocols* **1**:769–774 DOI 10.1038/nprot.2006.102.

Kim SK, Ryu SY, No J, Choi SU, Kim YS. 2001. Cytotoxic alkaloids from houttuynia cordata. *Archives of Pharmacal Research* **24**:518–521 DOI 10.1007/BF02975156.

Li GZ, Chai OH, Lee MS, Han EH, Kim HT, Song CH. 2005. Inhibitory effects of houttuynia cordata water extracts on anaphylactic reaction and mast cell activation. *Biological and Pharmaceutical Bulletin* **28**:1864–1868 DOI 10.1248/bpb.28.1864.

Lin CH, Chao LK, Lin LY, Wu CS, Chu LP, Huang CH, Chen HC. 2022. Analysis of volatile compounds from different parts of houttuynia cordata thunb. *Molecules* **27(24)**:8893 DOI 10.3390/molecules27248893.

Lü D, Xu P, Hou C, Li R, Hu C, Guo X. 2021. iTRAQ-based quantitative proteomic analysis of silkworm infected with Beauveria bassiana. *Molecular Immunology* **135**:204–216 DOI 10.1016/j.molimm.2021.04.018.

Lu HM, Liang YZ, Yi LZ, Wu XJ. 2006b. Anti-inflammatory effect of houttuynia cordata injection. *Journal of Ethnopharmacology* **104**:245–249 DOI 10.1016/j.jep.2005.09.012.

Lu H, Wu X, Liang Y, Zhang J. 2006a. Variation in chemical composition and antibacterial activities of essential oils from two species of Houttuynia THUNB. *Chemical and Pharmaceutical Bulletin* **54**:936–940 DOI 10.1248/cpb.54.936.

Ng LT, Yen FL, Liao CW, Lin CC. 2007. Protective effect of houttuynia cordata extract on bleomycin-induced pulmonary fibrosis in rats. *The American Journal of Chinese Medicine* **35**:465–475 DOI 10.1142/S0192415X07004989.

Pan L, Wan L, Song L, He L, Jiang N, Long H, Huo J, Ji X, Hu F, Fu J, Wei S. 2022. Comparative proteomic analysis provides new insights into the development of haustorium in taxillus chinensis (DC.) Danser. *BioMed Research International* **2022**:9567647.

Ramakrishnan V, White SW. 1998. Ribosomal protein structures: insights into the architecture, machinery and evolution of the ribosome. *Trends in Biochemical Sciences* **23**:208–212 DOI 10.1016/S0968-0004(98)01214-6.

Rogalski M, Schöttler MA, Thiele W, Schulze WX, Bock R. 2008. Rpl33, a nonessential plastid-encoded ribosomal protein in tobacco, is required under cold stress conditions. *The Plant Cell* **20**:2221–2237 DOI 10.1105/tpc.108.060392.

Smith PK, Krohn RI, Hermanson GT, Mallia AK, Gartner FH, Provenzano MD, Fujimoto EK, Goeke NM, Olson BJ, Klenk DC. 1985. Measurement of protein using bicinchoninic acid. *Analytical Biochemistry* **150**:76–85 DOI 10.1016/0003-2697(85)90442-7.

Verma RS, Joshi N, Padalia RC, Singh VR, Goswami P, Kumar A. 2017. Chemical composition and allelopathic, antibacterial, antifungal, and antiacetylcholinesterase activity of fish-mint (houttuynia cordatathunb.) from India. *Chemistry & Biodiversity* **14**:e1700189 DOI 10.1002/cbdv.201700189.

Řebíčková K, Bajer T, Šilha D, Houdková M, Ventura K, Bajerová P. 2020. Chemical composition and determination of the antibacterial activity of essential oils in liquid and vapor phases extracted from two different southeast asian herbs-houttuynia cordata (saururaceae) and persicaria odorata (polygonaceae). *Molecules* **25(10)**:2432 DOI 10.3390/molecules25102432.

Wilson DN, Doudna Cate JH. 2012. The structure and function of the eukaryotic ribosome. *Cold Spring Harbor Perspectives in Biology* **4**:a011536.

Wiśniewski JR, Zougman A, Nagaraj N, Mann M. 2009. Universal sample preparation method for proteome analysis. *Nature Methods* **6**:359–362 DOI 10.1038/nmeth.1322.

Wong CF, Poon CK, Ng TW, Pan HH, Khaw EC, Tsang KF, Mui YW, Lo YH, Hao MF, Ko CH. 2022. Anti-inflammatory, antipyretic efficacy and safety of inhaled Houttuynia cordata thunb. essential oil formulation. *Journal of Ethnopharmacology* **297**:115541 DOI 10.1016/j.jep.2022.115541.

Wu X, Li J, Wang S, Jiang L, Sun X, Liu X, Yao X, Zhang C, Wang N, Yang G. 2021a. 2-undecanone protects against fine particle-induced kidney inflammation via inducing mitophagy. *Journal of Agricultural and Food Chemistry* **69**:5206–5215 DOI 10.1021/acs.jafc.1c01305.

Wu Z, Deng X, Hu Q, Xiao X, Jiang J, Ma X, Wu M. 2021b. Houttuynia cordata thunb: an ethnopharmacological review. *Frontiers in Pharmacology* **12**:714694 DOI 10.3389/fphar.2021.714694.

Xu YW. 2012. Monoterpene secondary metablites in Houttuynia cordata Thunb. Doctor. SICAU.

You C, Chen L, He H, Wu L, Wang S, Ding Y, Ma C. 2017. iTRAQ-based proteome profile analysis of superior and inferior Spikelets at early grain filling stage in japonica Rice. *BMC Plant Biology* **17**:100 DOI 10.1186/s12870-017-1050-2.

Yu HD, Yang XF, Chen ST, Wang YT, Li JK, Shen Q, Liu XL, Guo FQ. 2012. Down-regulation of chloroplast RPS1 negatively modulates nuclear heat-responsive expression of HsfA2 and its target genes in Arabidopsis. *PLOS Genetics* **8**:e1002669 DOI 10.1371/journal.pgen.1002669.

Zhan C, Li X, Zhao Z, Yang T, Wang X, Luo B, Zhang Q, Hu Y, Hu X. 2016. Comprehensive analysis of the triterpenoid saponins biosynthetic pathway in anemone flaccida by transcriptome and proteome profiling. *Frontiers in Plant Science* **7**:1094.

Zhang P, Li C, Zhang P, Jin C, Pan D, Bao Y. 2014. iTRAQ-based proteomics reveals novel members involved in pathogen challenge in sea cucumber apostichopus japonicus. *PLOS ONE* **9**:e100492 DOI 10.1371/journal.pone.0100492.

Zhou K, Zhang C, Xia J, Yun P, Wang Y, Ma T, Li Z. 2021. Albino seedling lethality 4; Chloroplast 30S ribosomal protein S1 is required for chloroplast ribosome biogenesis and early chloroplast development in rice. *Rice* **14**:47 DOI 10.1186/s12284-021-00491-y.

Zhuang T, Li F, Huang LR, Liang JY, Qu W. 2015. Secondary metabolites from the plants of the family saururaceae and their biological properties. *Chemistry & Biodiversity* **12**:194–220 DOI 10.1002/cbdv.201300342.